

Polymer Matrix Composites Reinforcement with Nanoparticulate Rice Husk Ash

Nafisat Tijjani^{a*}, Mastura Shehu Tofa^b, Ibrahim Abdullahi^c, Auwal Salisu Yunusa^a, Ishaq Bala Adam^d.

^aDepartment of Mechatronics Engineering Technology, School of Technology, Kano State Polytechnic, Nigeria

^b40 NNDC Quarters, Hotoro GRA, Kano State, Nigeria.

^cDepartment of Mechanical Engineering, Faculty of Engineering, Bayero University Kano, Kano State, Nigeria.

^dDepartment of Mechanical Engineering Technology, School of Technology, Kano State Polytechnic, Nigeria.

Corresponding email: *nafisattijjani19@gmail.com

Article information

Article History

Received 24 April 2023

Revised 4 May 2023

Accepted 8 May 2023

Available online 12 June 2023

Keywords:

Polymer Matrix Composite, Rice Husk Ash, Nanoparticles, Ultimate Tensile Strength, Flexural Strength.

OpenAIRE

<https://doi.org/10.5281/zenodo.8024735>

<https://nipes.org>

© 2023 NIPES Pub. All rights reserved

Abstract

Polymer matrix composites (PMC) provide improved mechanical properties when compared to unreinforced polymers. Consequently, they are widely used as structural materials for different engineering applications. Rice husk is an agricultural waste found in abundance that can be utilised as reinforcing material when incinerated. This paper investigates the effect of addition of small quantity of nanoparticulate rice husk ash (RHA) in plastic for strength enhancement. X-Ray Fluorescence (XRF) Technique was used to determine of the chemical composition of the RHA. Micrographs of the RHA were produced using Scanning Electron Microscope (SEM), and ImageJ software was used for characterisation of the particles. RHA nanoparticles having mean diameter of 21nm were used for the composite production. Composites test samples were produced by manual mixing with 2 wt%, 4 wt%, 6 wt%, 8 wt% and 10 wt% RHA reinforcement, in cast iron mould. The mixing ratio for the composite samples were 0-10 wt% added at 2 wt% interval, and 5:1 catalyst-accelerator mixing ratio. Methyl ethyl ketone peroxide (MEKP) was used as catalyst, and cobalt naphtholate as accelerator. The test samples were subjected to tensile strength tests and flexural strength tests. The results from the tests carried out showed maximum improvement of Ultimate Tensile Strength (UTS), Tensile Modulus (TM) and Modulus of Rupture (MOR) at 2 wt% RHA reinforcement when compared with the unreinforced polyester. A decrease in the value of the properties was observed with further increase in RHA composition in the PMC

1. Introduction

Composites are two or more materials combined with the intent of getting a unique material or desirable properties of the constituent materials such that the property cannot be found in a single naturally existing material [1-4]. According to Subrahmanya et al. [5], composites are broadly

classified based on type of matrix as Polymer Matrix Composites (PMC), Ceramic Matrix Composites (CMC) and Metal Matrix composites (MMC). The Polymer Matrix Composites (PMC) are made up of different types of organic polymers. They consist of short or continuous fibers with the several reinforcing agents. The matrix in PMC adheres the fibers together for transfer of load between them such that mechanical loads are supported by the fibers. Consequently, mechanical properties such as fracture toughness, high strength and stiffness are improved. Moreover, PMC reinforced with natural fibers have a higher resistance and interfacial bonding between them, which helps to maintain their chemical and mechanical identities. Formation of composites can be facilitated with the aid of a catalyst and an accelerator. The accelerators are used in small quantities to enhance the efficiency of catalyst. Hussain et al. [1] explained that different techniques can be used for formation of composites using the combination of a binder and a reinforcement material. Some of the techniques use close moulds, as found in Resin Transfer Moulding (RTM) technique, while use of open moulds is adopted in some others, such as the Wet lay-up and the Vacuum Resin Transfer Moulding (VARTM) techniques. On the other-hand, for formation of contours of complex forms and high-quality complex structures, the Fiber Placement and Autoclave Processing techniques are used respectively. To obtain good nanoparticle arrangement and dispersion at low cost in large volume, the Pultrusion production process can be adopted.

Several studies [6-8] have identified some techniques that are used for characterization and measurement of nanoparticles. These are; the Scanning Electron Microscopy (SEM), the Transmission Electron Microscopy (TEM), X-ray Diffractometry (XRD), and the Small Angle X-ray Scattering (SAXS). They further explained that the SEM and the TEM can measure nanoparticles down to 1 nm. Din et al. [9] further added that, other advanced techniques such as the Atomic Force Microscopy (AFM), Scanning Tunnelling Microscopy (STM), Fourier Transformed Infrared Spectroscopy (FTIR), X-ray Photoelectron Spectroscopy (XPS), Nuclear Magnetic Resonance (NMR), and Differential Scanning Calorimetry (DSC) have also been used recently for quantitative characterization of nanoparticles in nanocomposites.

Rapid growth especially in the manufacturing industries has led to the demand for materials with improved properties in terms of strength, stiffness, low cost of production and sustainability. Choice of materials to a great extent has been influenced by right combination of desirable properties for a specified application. For instance, in construction applications, an efficient, durable, and cost-effective material is preferred. In the work of English [10], wood fiber-plastic composite formed was more durable than wood material alone. Stiffness also improved with addition of wood content to plastic matrix. By encapsulating wood in a plastic matrix, it is protected from unfavorable environmental conditions such as moisture that may cause damage to it. English [10] further pointed that the composite is less affected by variations in humidity when compared with plain wood. It is economical as it can be produced from wood waste and can be recycled, and the problem of wood waste disposal is also eliminated.

Hybrid composites can be used for reinforcement. Borba et al. [11] demonstrated the use thermoplastic elastomers; styrene-butadiene-styrene triblock copolymer (SBS) matrix for reinforcement with Curaua fiber and nanoparticulate mineral (montmorillonite clay, MMT). The mechanical performance of the hybrid composite showed best improvement with 2 wt% MMT and 5 wt% Curaua fiber. Further increase in the fiber only resulted in drop of tensile strength. Improvement in tensile and flexural strength is sometimes accompanied with a drop in impact strength [12]. However, Morais et al. [13] discovered that impact resistance can be improved simultaneously with tensile and flexural strengths by use of thermoplastic composite, where one

polymer is able to absorb impact energy. Morais et al. [13] used Curaua fiber for reinforcement of a combination of ethylene-vinyl acetate (EVA) and high-density polyethylene (HDPE). The result showed improved tensile and flexural strengths simultaneously with enhanced impact resistance. Fillers and fibers generally improve high strength modulus requirements in composites. Fibers can be natural or synthetic. The natural fiber can come from plants and are cellulose based; such as cotton and flax, or from animals and are protein based; such as wool and silk [5]. Though composites, especially those formed with inorganic nanoparticles such as quantum dots, metal oxides, ceramic and metallic nanoparticles mainly improve mechanical performance [14], natural fibers possess more economic advantages [15]. Natural fibers are also lightweight, renewable, and biodegradable.

Surface treatment has been found to have some effects on mechanical properties of natural fiber composites. According to Latif et al. [16], interfacial bonding and crystallinity index govern mechanical properties in the natural fiber composites. Latif et al. [16] further added that, removal of non-cellulose compounds by dissolution chemical treatments such as mercerization and acetylation from the surface of these composites facilitates the interfacial bonding between the reinforcing and matrix phase in the composites which overall improves the tensile and flexural properties, and the impact strength of the composites.

Recent researches have shown that decrease in particle size of fillers in composites promote improved interfacial bonding between matrix and fillers [12]. General development in composites has been decrease in size of filler material; from macro to meso and micro to nano. The field of nanotechnology has gained significant attention for wide applications in different fields such as medicine, agriculture and Food production, construction, automobile, and electrical industries [9], [15], [17], [18]. Din et al. [9] further explained that PMC, CMC, and MMC, are also sub-categorized as Polymer Matrix Nanocomposites (PMNC), Ceramic Matrix Nanocomposites (CMNC), and Metal Matrix Nanocomposites (MMNC) when they are formed from nanoparticles respectively. The PMNC, the CMNC, and the MMNC present enhanced properties when compared with composites fabricated at the micro scale. Significant improvements have been observed in optical property, electrical and thermal conductivity, surface appearance and good barrier for gases, on addition of nanoparticles in composites [19]. Addition of nanoparticles in small quantities as reinforcement has shown observable effects and improvements on physical and mechanical properties of composites. Miscibility and morphology is modified in polymer nanocomposites [18].

Plant fibres from common agricultural waste are found to be suitable for reinforcing plastics due to their low density, low cost, high strength and stiffness characteristics. In order to reduce the cost of the production, Yap et al. [15] suggested the use of waste material as fillers in composites. The use of abundant agricultural wastes to produce environment-friendly materials can serve as an alternative. With a total rice production of the world estimated to about 495.9 metric tons as of 2018/2019, with approximately 123.87 metric tons of rice husk produced, the use of rice husk has a great potential. Furthermore, rice husk being one of the abundant agricultural wastes when incinerated or openly disposed, poses great danger to human health and the environment. To reduce such negative effect, rice husk can be utilised in production of composites. According to Yap et al. [15], biodegradable polymers used for composite formation show observable changes and improvements in tensile strength, Young's modulus, and elongation at break. Incorporating rice husk as a substitute for starch based biodegradable polymer gave even better mechanical properties.

Recently, there is increasing research on nanoparticulate rice husk ash. Among are the works of Alhadhrami et al. [20] and Nhung et al. [21]. However, much of the researches conducted lay emphasis on analysis and synthesis of nanoparticulate rice husk ash. There is a general agreement by researchers that there is great potential for the use of rice husk ash as nanofiller in composites for their abundance, cost-effectiveness, and favourable properties.

2.0 Materials and Methods

2.1 Materials and Equipment

The materials used for the production of the plastic composite are: polyester resin, rice husk, Methyl ethyl ketone peroxide (MEKP), and Cobalt-naphtholate. The Rice Husk was sourced from Kura Local Government Area of Kano State, Nigeria. The Polyester resin serves as the matrix, the rice husk ash as serves as the filler, Methyl ethyl ketone peroxide (MEKP) as catalyst, and Cobalt-naphtholate as accelerator. The proportion of the matrix and filler is taken at 0 wt%, 2 wt%, 4 wt%, 6 wt%, 8 wt% and 10wt% of RHA. While the catalyst to accelerator ratio was 5:1.

The equipment used for the preparation of the polymer matrix composite are: the furnace, the mortar and pestle, the weighing balance, micrometer screw gauge, a lint free cloth, distilled water, a measuring cylinder, cast-iron mould, a Universal Testing Machine (Cussons Technology P5030), a mechanical sieving machine, and a Laboratory ball mill (BICO-395-50 12INDRUM 3PH). While for the chemical analysis the X-Ray Florescence machine (Thermo scientific Advant'X 1200 Model), and Scanning Electron Microscope (BOC Edwards K950X) used, with ImageJ for characterisation of the particles.

2.2 Rice Husk Ash Preparation

The Rice husk was manually blown to remove dirt, stones and rice particles from the husk. The husk was completely burnt to ashes in a furnace at 700⁰C for 4 hours. After cooling, the ash was ground using mortar and pestle, sieved to 75 μ m and 2kg of the RHA was further ground for 11hours in Bico Ball Mill with 285 iron balls of 20kg running at 450rpm (revolutions per minute) with a balls charge ratio of 10:1 to obtain the RHA nanoparticulates.

2.3 RHA Chemical Composition and Characterization

Chemical composition and characterization of the RHA nanoparticles was carried out after obtaining the RHA nanoparticles. The RHA particles were first viewed under scanning electron microscope after ball milling, and micrographs were produced. The particles were then characterized using imageJ.

The X-Ray Fluorescence (XRF) Technique was used to determine of the chemical composition of the RHA. The RHA was first pulverized, then pelletized before being loaded in the XRF machine for twenty minutes, after which data generated is collated automatically on the computer attached to the XRF machine.

2.4 Polymer Matrix Composite Preparation and Analysis

The composite was prepared using stir mixing technique. It was produced in a cast iron mould using the nanoparticulate RHA as reinforcement, and matrix of polyester resin along with methyl ethyl ketone peroxide (MEKP) as catalyst and cobalt naphtholate as accelerator. The RHA was added and mixed in the composite samples from 0 -10 wt% addition at 2 wt% interval, and 5:1 as the catalyst-accelerator mixing ratio. The morphology of the nanoparticulate RHA was analysed using micrographs produced by the Scanning Electron Microscope (SEM). The RHA nanoparticles

are sputter coated to make a thin conductive cover for high quality imaging. The SEM gave high resolution by using electromagnets in place of lenses. It used electron instead of light to form images and allowed much control over the degree of magnification.

2.5 Strength Tests

Two different tests for strength were conducted in this work; the Flexural strength tests and Tensile strength tests. For each of the two tests, there is a varied wt% of RHA from 0-10 wt%, at an interval of 2 wt%. This means that the tests were carried-out at 0 wt%, 2wt%, 4 wt%, 6 wt%, 8 wt%, and 10 wt% RHA, and for every wt% variation of RHA, the test was conducted with five different samples. Thus, a total of 60 samples were produced; 30 samples for tensile strength tests, and 30 samples for flexural strength tests. 5 samples each for tests at 0 wt%, 2 wt%, 4 wt%, 6 wt%, 8 wt% and 10 wt% of RHA for the two different test.

Flexural Strength Test: A three-point loading system test was employed according to ASTM D-790 standard [22] to determine the flexural properties of the composites. Rectangular specimens of size 130mm by 20mm by 5mm were subjected to strain rate of 0.1mm/mm/min and span length of 80mm on a Universal testing machine. The test was terminated for each sample at break and the modulus of rupture was calculated using the values obtained.

Tensile Strength Test: Tensile strength test was conducted following the ASTM D638-02 standard [23]. Dumbbell shaped specimens of thickness 4.1mm, original width of 18.5mm and original distance between gauge marks of 78.5mm were used. The Ultimate Tensile Strength (UTS), the percentage elongation at break ($\%EL_b$) and the Young's modulus or tensile modulus (E) of the samples were determined [24].

3.0 Results and Discussion

The RHA particles appeared to be spherical in shape, and some of the particles which appeared boldly are shown with the arrows in figure 1 below:

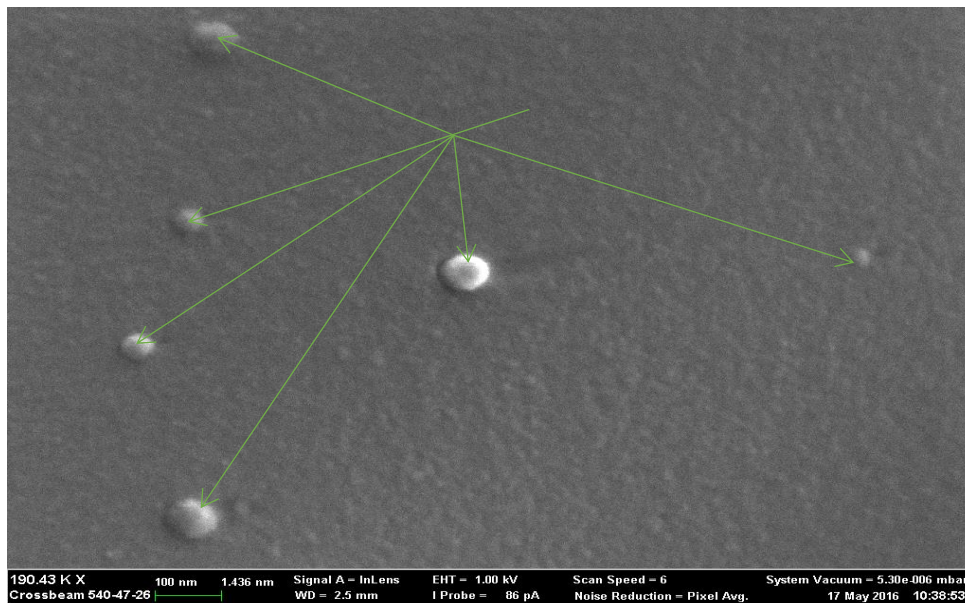


Figure 1: A Micrograph Showing Spherical Nature of the Rice Husk Ash Particles

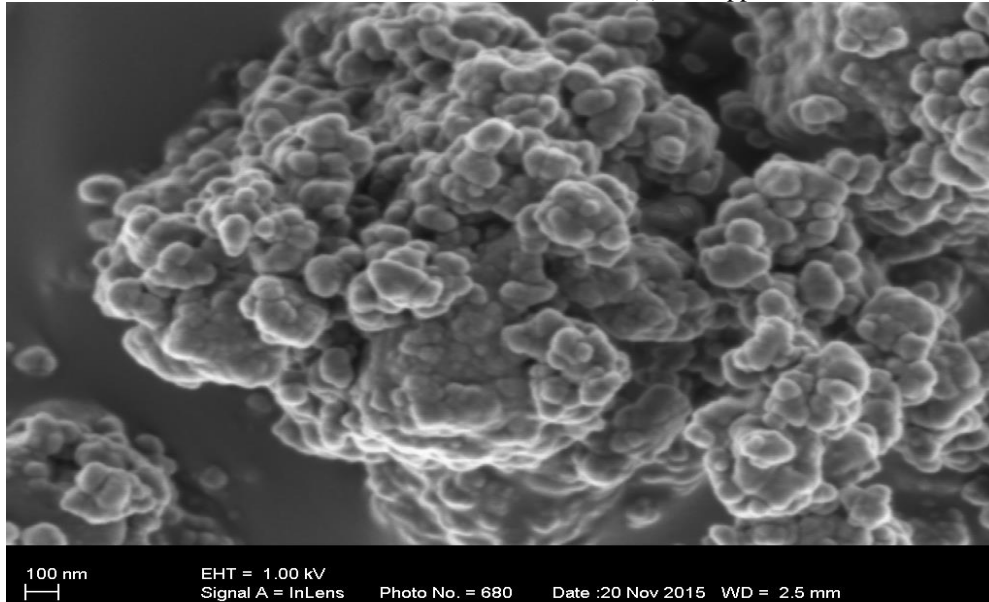


Figure 2: RHA Nanoparticles Micrograph

The characteristics obtained from the micrograph using the ImageJ, are tabulated below:

Table 1: RHA Particles Size Characterization Result

Characteristic	Area of Particle (nm ²)	Circularity	Aspect Ratio	Roundness	Solidity
Mean	1467.63	0.578	2.146	0.558	0.735

Figure 2 was used for the particle characterisation and the results shown in Table 1. Imputing value of the mean area of particles from table 1 above in formula for calculating area of sphere, the mean diameter of the RHA particles was found.

Area of RHA particle, $A = \pi d^2$

Where d is the mean diameter of RHA particle

And $\pi = 3.1415$

Therefore; $d = \sqrt{\frac{A}{\pi}}$

Imputing the values for A and π

$$d = \sqrt{\frac{1467.63}{\pi}}$$

$$d \approx 21nm$$

The chemical composition of the RHA determined by X-Ray Fluorescence (XRF) is tabulated below:

Table 2: Chemical Composition of Rice Husk Ash

S/No.	Chemical composition	Percentage
1	SiO ₂	87.22
2	K ₂ O	1.12
3	CaO	2.12
4	Al ₂ O ₃	0.70
5	MgO	1.18
6	Fe ₂ O ₃	1.68
7	NiO	0.20
8	MnO	1.06
9	P ₂ O ₅	0.87
10	TiO ₂	0.46
11	S	0.04
12	ZrO ₂	0.01
13	Cr ₂ O ₃	0.03
14	LOI	1.06
15	Others	2.25

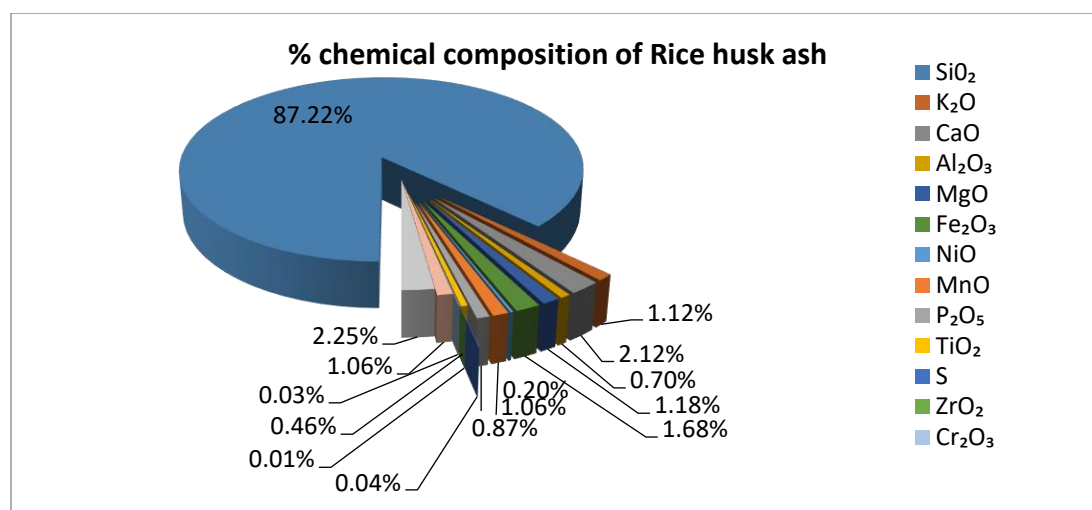


Figure 3: Rice Husk Ash Chemical Composition

3.1 Flexural Strength Test

The Flexural Strength or modulus of rupture (MOR) was calculated at break for each sample using:

$$MOR, \sigma_{fm} = \frac{3PL}{2bd^2}$$

Where:

σ_{fm} = Flexural strength (MPa)

P = Load (Force) at break (N)

L = Support span (mm)

b = width of sample (mm)

d = depth or thickness of sample (mm)

The values of Force and Deformation at breaking were obtained from the tests, and the MOR of all the samples was calculated and the results tabulated below:

Table 3: Flexural Test Results of Various Compositions of Nanoparticulate RHA Plastic Composite

RHA wt%	Sample Number	Force at peak (kgf)	Deformation at Break (mm)	Modulus of Rupture (Mpa)	Average Modulus of Rupture (Mpa)
0	1	30.082	3.723	70.800	44.256
	2	9.1775	0.949	21.599	
	3	21.108	2.357	49.680	
	4	16.825	2.048	39.600	
	5	16.825	1.328	39.600	
2	1	21.516	1.314	50.640	46.224
	2	23.963	2.176	56.400	
	3	18.049	1.123	42.480	
	4	15.806	1.115	37.200	
	5	18.865	1.601	44.400	
4	1	16.825	2.037	39.600	32.640
	2	15.194	1.810	35.760	
	3	9.789	0.830	23.040	
	4	12.848	0.925	30.240	
	5	14.684	1.115	34.560	
6	1	6.832	0.550	16.080	18.528
	2	9.687	1.203	22.800	
	3	9.177	0.896	21.600	
	4	9.585	0.731	22.560	
	5	4.079	0.382	9.600	
8	1	5.914	0.535	13.920	16.176
	2	9.177	0.890	21.600	
	3	7.546	0.807	17.760	

	4	6.628	0.602	15.600	
	5	5.099	0.570	12.000	
10	1	8.260	0.959	19.440	12.672
	2	3.365	0.428	7.920	
	3	7.852	0.992	18.480	
	4	3.161	0.346	7.440	
	5	4.283	0.638	10.080	

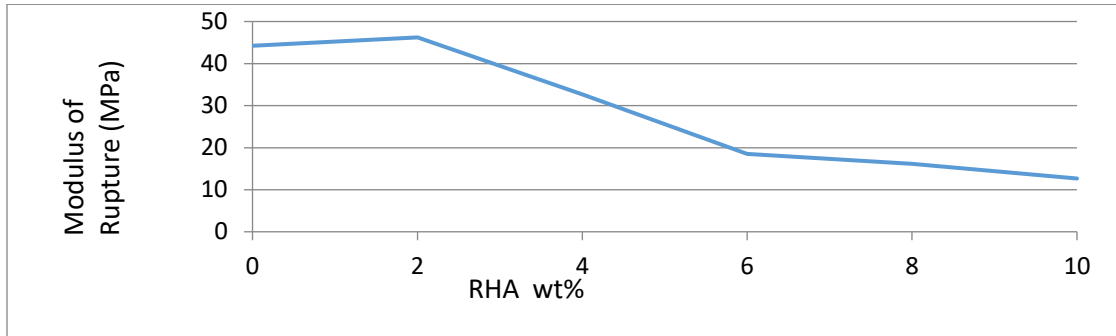


Figure 4: Modulus of Rupture (MPa) Against RHA wt% Loading

From the results in Table 4, the average value of MOR for the composite ranged from 46.22 MPa to 12.67 MPa with the unreinforced polyester having 44.26 MPa. A slight improvement of MOR has been observed in the composite with 2 wt% RHA, and a decline with further increase in RHA content.

3.2 Tensile Strength Test

The tensile stress at break or the Ultimate Tensile Strength (UTS) was calculated as:

$$UTS = \frac{P}{b_o \times d_o}$$

Where:

P = load at break of composite specimen (N)

b_o = original width of composite (mm)

d_o = original thickness of composite (mm)

From the tensile test results, Young's modulus or tensile modulus (E) was calculated as follows:

$$E = \frac{uts}{\varepsilon}$$

Where:

uts = ultimate tensile strength

ε = strain

And percentage elongation at break ($\%EL_b$) was calculated as:

$$\%EL_b = \frac{L - L_o}{L_o} \times 100 \quad (9)$$

Where;

L = distance between gauge mark at break

L_o = original distance between gauge marks

Ultimate tensile strength (UTS) for sample 1 of 0wt% RHA was calculated using equation.

$$UTS = \frac{P}{b_o \times d_o}$$

$$UTS = \frac{85.8 \times 9.80665}{18.5 \times 10^{-3} \times 4.1 \times 10^{-3}} = 11.071 MPa$$

Similarly, UTS for all the other samples were calculated and the results tabulated below.

Young's modulus or tensile modulus (E) was calculated using equation:

$$E = \frac{uts}{\varepsilon}$$

strain, $\varepsilon = \frac{L - L_o}{L_o}$ but $L - L_o$ is elongation at break

$$\varepsilon = \frac{1.314}{78.5} = 0.017$$

$$E = \frac{uts}{\varepsilon} = \frac{11.071}{0.017} = 661.407 MPa$$

And percentage elongation at break ($\%EL_b$) was calculated using the equation:

$$\begin{aligned} \%EL_b &= \frac{L - L_o}{L_o} \times 100 \\ &= \frac{1.314}{78.5} \times 100 = 1.674\% \end{aligned}$$

Similarly, strain, %EL and TM were calculated for all the other samples and results were tabulated in Table 5.

Table 4: Tensile Test Result of Various Compositions of Nanoparticulate RHA Plastic Composite

RHA wt%	Sample Number	Load at Break (kgf)	Elongation at Break (mm) $L - L_o$	% Elongation at break	Ultimate Tensile Strength (MPa)	Strain E	Tensile Modulus (MPa)
0	1	85.800	1.314	1.674	11.071	0.017	661.407
	2	75.100	1.520	1.936	9.691	0.019	500.464
	3	67.600	1.532	1.952	8.723	0.013	670.981
	4	61.200	1.378	1.755	7.897	0.018	449.862
	5	75.300	1.140	1.452	9.716	0.015	669.063
2	1	92.200	1.733	2.208	11.897	0.022	538.901
	2	85.100	1.248	1.590	10.981	0.016	690.704
	3	101.600	2.379	3.031	13.110	0.030	432.590
	4	82.903	1.292	1.646	10.697	0.016	649.957
	5	92.284	1.052	1.340	11.908	0.013	888.561
4	1	72.400	1.446	1.842	9.342	0.018	507.162
	2	70.100	2.209	2.814	9.045	0.028	321.439
	3	67.200	1.670	2.127	8.671	0.021	407.596
	4	71.200	1.187	1.512	9.187	0.015	607.584
	5	88.400	2.619	3.336	11.407	0.033	341.896
6	1	61.200	2.818	3.590	7.897	0.036	219.982
	2	51.600	1.299	1.655	6.658	0.017	402.362
	3	58.500	1.145	1.459	7.549	0.015	517.520

	4	73.000	2.150	2.739	9.420	0.027	343.923
	5	74.900	2.011	2.562	9.665	0.026	377.265
8	1	63.900	2.010	2.561	8.245	0.026	322.019
	2	68.000	2.260	2.879	8.774	0.029	304.774
	3	56.500	1.248	1.590	7.290	0.016	458.575
	4	54.963	2.091	2.664	7.092	0.027	266.252
	5	60.500	2.880	3.669	7.807	0.037	212.784
10	1	43.600	1.877	2.391	5.626	0.024	235.288
	2	51.700	1.660	2.115	6.671	0.021	315.471
	3	28.800	1.100	1.401	3.716	0.014	265.202
	4	45.683	3.815	4.860	5.895	0.049	121.293
	5	33.100	0.553	0.704	4.271	0.007	606.289

Table 5: Summary of Tensile Test Result of Various Compositions of Nanoparticulate RHA Plastic Composite

RHA wt%	Average force at peak (kgf)	Average Elongation at Break (mm)	Average Ultimate Tensile Strength (Mpa)	Average Percentage Elongation (Mpa)	Average Tensile Modulus (Mpa)
0	73.000	1.377	9.420	1.754	577.342
2	90.817	1.541	11.719	1.963	640.142
4	73.860	1.826	9.531	2.326	441.147
6	63.840	1.885	8.238	2.401	375.626
8	60.773	2.098	7.842	2.672	315.752
10	40.577	1.801	5.236	2.294	311.542

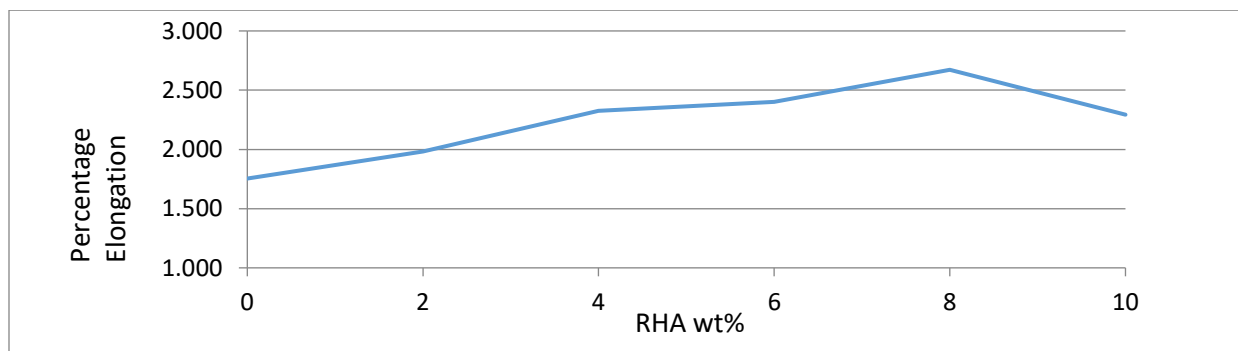


Figure 5: Percentage Elongation (%) against RHA wt% Loading

Figure 5 indicates that percentage elongation of the reinforced composites were greater than that of unreinforced samples. The percentage elongation was found to continuously increase with

increase in RHA wt% loading from 1.75% of the unreinforced sample to a maximum of 2.67% at 8 wt% RHA, with a decline from 2.67% at 8 wt% RHA to 2.29% at 10 wt% RHA loading. It can be suggested that the increase in RHA helps support stress absorbed by the matrix, hence the increase in percentage elongation with increase in RHA wt% loading.

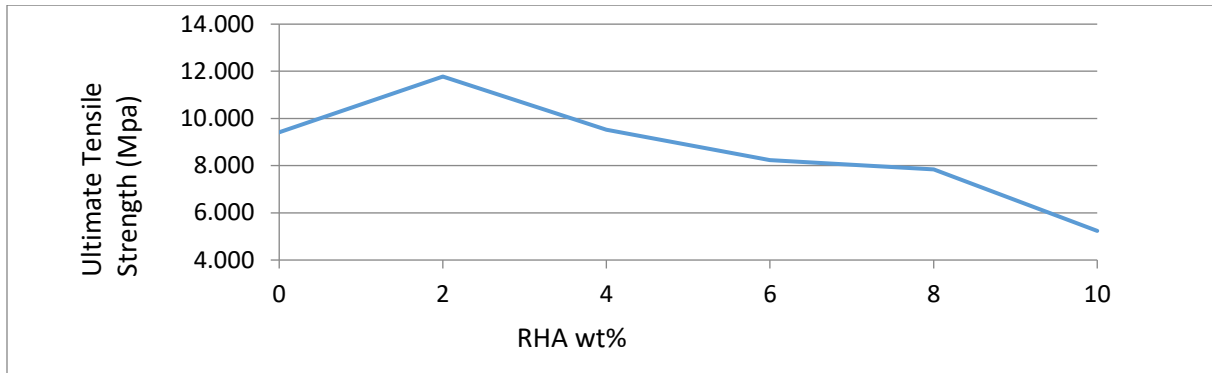


Figure 6: Ultimate Tensile Strength (MPa) against RHA wt% Loading

Ultimate Tensile Strength (UTS), increased from 9.420 Mpa at 0 wt% RHA, to 11.719 Mpa at 2 wt% RHA. There is a sharp decline in the UTS with further increase in RHA wt% loading, thus suggesting best spatial distribution of RHA with a 2 wt% RHA content. This can be attributed to the characteristic of Rice Husk which is easy agglomeration and the weak interface between filler and matrix, which cause more filler particle clusters at higher filler loading. Thus, UTS was found to be highest at 2 wt% RHA loading with a value of 11.719 Mpa. With increase in RHA wt% loading, decrease in UTS is realised. Decrease in strength of composites is associated with high content of filler material in works [25], [26], [27].

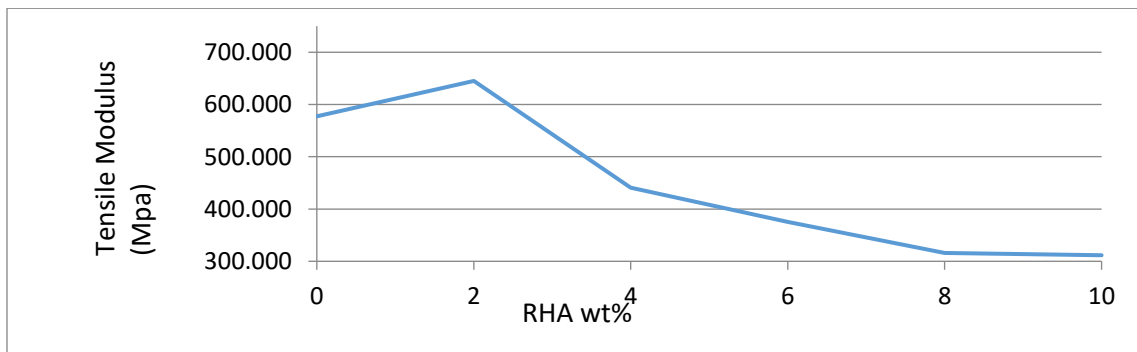


Figure 7: Tensile Modulus (MPa) against RHA wt% Loading

Figure 7 shows that the TM improved at 2 wt% RHA loading when compared with the unreinforced polymer. TM is highest at 2 wt% RHA loading with a value of 640.142 Mpa. This shows that stiffness has improved with 2 wt% RHA. A sharp decline was observed with further increase in RHA content. This decline is likely due to filler particle clustering.

3.3 Contrast between strength properties of Unreinforced and Reinforced Polymer Matrix Composite

From the strength tests conducted and the results obtained, the table below presents values of the strength properties of the pure cast (Unreinforced) polyester and the reinforced PMC. It also gives the maximum value the properties and wt% of RHA at that value.

Table 6: Contrast between strength properties of Unreinforced and Reinforced Polymer Matrix Composite

Properties	Values for Pure Cast (Unreinforced) Polyester	Maximum Values for Reinforced PMC	wt% of RHA at Maximum Values for Reinforced PMC
Ultimate tensile strength (MPa)	9.420	11.719	2.000
Percentage Elongation at break (%)	1.754	2.672	8.000
Tensile Modulus (MPa)	577.342	640.142	2.000
Modulus of Rupture (MPa)	44.256	46.224	2.000

4.0 Conclusions

The mechanical properties test results showed significant improvement of Ultimate Tensile Strength (UTS), Tensile Modulus (TM) and Modulus of Rupture (MOR) at 2 wt% RHA reinforcement when compared with the unreinforced polyester, and a decline with further increase in RHA content. The samples with 2 wt% RHA were found to have UTS of 11.719 MPa, TM of 640.142 MPa and MOR of 46.224 MPa. Therefore, it can be concluded that to improve the strength the PMC using nanoparticulate RHA, a small quantity of RHA (2 wt% RHA) is sufficient. Several researchers have agreed that the morphology of materials has significant influence on their strength, and mechanical properties in general [7], [15]. Composite's microstructure will show any spatial distribution or clustering of the RHA content in the PMC at varying load. This will make it possible to draw conclusions on the influence of the structural arrangement of RHA nanoparticles in the composite on the strength on the PMC. Hence, it is recommended that future research is conducted on analysis of microstructure on nanoparticulate RHA PMC.

References

- [1] F. Hussain, H. Mehdi, O. Masami and E. G. Russel. (2006). "Polymer Matrix Nanocomposites, Processing, Manufacturing and Applications: An Overview." *Journal of composite materials*. vol. 40, no. 17, pp. 1555-1557. Available: <https://doi.org/10.1177/0021998306067321>

- [2] H. Thomas and V. S. Dorothee. (2010). "Polymer Nanoparticles Composites: from synthesis to modern applications." *Journal of material chemistry and physics*, vol. 3, no. 6, pp. 3468-3517. Available: <https://www.mdpi.com/1996-1944/3/6/3468>
- [3] S. D. Maulida and B. Faisal. (2015). "The tensile strength properties effect of rice husk ash as on the composite of plastic drinking bottle." *International Journal of Science and Technology Research*, vol. 4, no. 4, pp. 66-69. Available: <https://www.ijsr.net/archive/v5i5/NOV163445.pdf>
- [4] W. D. Callister, D. G. Rethwisch and R. Balasubramaniam, *Callister's Material Science and Engineering*, 2nd ed. New Delhi: Wiley, 2014.
- [5] K. Subrahmanya, T. G. Yashas, M. R Sanjay, P. Madhu, P. SenthamaraiKannan and B. Yogesha. (2018). "Polymer Matrix-Natural Fiber Composites: An Overview." *Cogent Engineering*, vol. 5, no. 1, pp. 1-13. Available: <https://www.tandfonline.com/doi/full/10.1080/23311916.2018.1446667>
- [6] D. J. Burleson, M. D. Driessen, and R. L. Pen. (2004). "On the Characterisation of Environmental Nanoparticles." *Journal of Environmental Science and Health*, vol. 39, no. 10, pp. 2707-2753 Available: <https://doi.org/10.1081/ESE-200027029>
- [7] H. Clemens, S. Mayer, and C. Scheu, "Microstructure and Properties of Engineering Materials: From Fundamentals to Applications." in *Neutrons and Synchrotron Radiation in Engineering Materials Science: From Fundamentals to Application*, 2nd ed, S. peter, S. Andreas, H. Clemens, S. Mayer, Eds. New Jersey: Wiley-VCH, 2017, pp. 1-20.
- [8] F. Joel and M. Vikas, *Synthesis of Polymer Nanocomposite: Review of Various Techniques*. New Jersey: Wiley- VCH, 2015.
- [9] S. H. Din, M. A. Shah, N. A. Sheikh, and M. Mursaleen. (2019). "Nano-Composites and their Applications: A review. Characterization and Application of Nanomaterials." *Enpress Publishers LLC*, vol. 2, No. 1. Available: <http://dx.doi.org/10.24294/can.v2i1.875>
- [10] B. English, "Use of Recycled Wood and paper in Building Applications," in *National Conference on Wood Transportation Structures*, Madison, Wisconsin, 1996.
- [11] P. M. Borba, A. Tedesco, and D. M. Lenz. (2014). "Effect of Reinforcement Nanoparticles Addition on Mechanical Properties of SBS/Curauá Fiber Composites." *Journal of Materials Research*, vol. 17, no. 2. Available: <https://doi.org/10.1590/S1516-14392013005000203>
- [12] K. Zdiri, A. Elamri, M. Hamdaoui, O. Harzallah, N. Khenoussi, and J. Brendle. (2018). "Reinforcement of Recycled PP Polymers by Nanoparticles Incorporation." *Green House Chemistry Letters and Reviews*, vol. 11, no. 3, pp. 296-311. Available: <https://doi.org/10.1080/17518253.2018.1491645>
- [13] J. A. De Moraes, R. Gadioli, and M-A. De Paoli. (2016). "Curaua fiber reinforced high-density polyethylene Composites: Effect of Impact Modifier and Fiber Loading." *Polimoros*, vol. 26, no. 2, pp.115-122. Available: <https://doi.org/10.1590/0104-1428.2124>
- [14] A. M Diez-Pascual. (2019). "Nanoparticle Reinforced Polymers." *Polymers*, vol. 11, no. 4, pp.625. Available: <https://doi.org/10.3390/polym11040625>
- [15] S. Yap, S. Sreekantan, M. Hassan, K. Sudesh and M. T. Ong. (2021). "Characterization and Biodegradability of Rice Husk-Filled Polymer Composites." *Polymers*, vol. 13, no. 1, pp. 104. Available: <https://doi.org/10.3390/polym13010104>
- [16] R. Latif, S. Wakeel, N. Z. Khan, A. N. Siddiquee, S. L. Verma, and Z. A. Khan. (2019). "Surface Treatments of Plant Fibers and their effects on Mechanical Properties of Fiber-Reinforced Composites: A Review." *Journal of Reinforced Plastics and Composites*, vol. 38, no. 1, pp. 15-30. Available: <https://doi.org/10.1177/0731684418802022>
- [17] F. P. La Mantia and M. Morreal. (2011). "Green Composite: A brief review." *Composites Part A: Applied Science and Manufacturing*, vol. 42, no. 6, pp. 579-588. Available: <https://doi.org/10.1016/j.compositesa.2011.01.017>
- [18] R. A. Ilyas, N. M Nurazzi, and M. N. E Nurorrrahim. (2022). "Fiber-Reinforced Polymer Nanocomposites." *Nanomaterials*, vol. 12, no. 17. Available: <https://doi.org/10.3390/nano12173045>
- [19] F. C. Leandro, P. V. Omar, A. C Marco, B. R. Marley, and R. M. Jose. "Modelling the Young Modulus of Nanocomposites: Neural Network Approach." in *Neural Networks International Joint Conference*, San Jose, 2011.
- [20] A. Alhadhrami, G. G. Mohamed, A. H. Sadek, S. H. Ismail, A. A. Ebnalwaled, and A. S. A. Almalki. (2022). "Behavior of Silica Nanoparticles Synthesized from Rice Husk Ash by the Sol-Gel Method as a Photocatalytic and Antibacterial Agent." *Materials*, vol. 15, no. 22. Available: <https://doi.org/10.3390/ma15228211>

- [21] D. T. T. Nhung, T. Hoa, N. T. A. Trinh, D. V. Phu, P. D. Tuan, and N. Q. Hien. (2017). "Synthesis of silica nanoparticles from rice husk ash." *Science and Technology Development Journal*, vol. 20, no. K7. pp. 50-54 Available: <http://dx.doi.org/10.32508/stdj.v20iK7.1211>
- [22] *Standard Test Method for Flexural Properties of Unreinforced and Reinforced Plastics and Electrical Insulating materials*, ASTM D790-17, 2017.
- [23] *Standard Test Method for Tensile Properties of Plastic*, ASTM D638-14, 2015.
- [24] S. S. Murugan. (2020). "Mechanical Properties of Materials: Definition, Testing and Application." *International Journal of Modern Studies in Mechanical Engineering*, vol. 6, no. 2, pp. 28-38. Available: <https://www.arcjournals.org/pdfs/ijmsme/v6-i2/3.pdf>
- [25] M. G. Eva, W. Basuki, B. Nurdin and A. Harry. "Preparation and Characterisation of Rice Husk Ash as Filler Material into Nanoparticles on HDPE thermoplastic composite." *Journal of Chemistry and material research*, vol. 6, no. 7, pp. 14-25, 2014.
- [26] Q. Wu, Y. Lei, F. Yao, Y. Xu and K. Lian, "Properties of HDPE/Clay/wood nanocomposites." *Journal of plastic Technology*, vol. 27, pp. 108-115, 2017.
- [27] Z. A. Kusmono, I. Mohd, W. Chow, S. Takeichi and T. Rochmadi. (2008). "Enhancement of Properties of PA6/PP Nanocomposites via Organic Modification and Compatibilization." *Express Polymer Letters*, vol. 2, no. 9, pp. 655-664. Available: <http://dx.doi.org/10.3144/expresspolymlett.2008.78>